J Mater Sci (2016) 51:2643–2652
DOI 10.1007/s10853-015-9578-8

Detailed dynamic rheological studies of multiwall carbon nanotube-reinforced acrylonitrile butadiene styrene composite

Jeevan Jyoti[1,2] · Bhanu Pratap Singh[1,2] · Sheetal Rajput[1] · Vidya Nand Singh[2,3] · S. R. Dhakate[1,2]

Received: 5 August 2015 / Accepted: 8 November 2015 / Published online: 30 November 2015

Abstract Dynamic rheological properties of multiwalled carbon nanotubes-(MWCNTs) reinforced acrylonitrile butadiene styrene (ABS) composites prepared by micro twin-screw extruder with back flow channel (used for proper dispersion) are reported. Scanning electron microscopic and high-resolution transmission electron microscopic studies showed that the nanotubes were uniformly dispersed in the ABS polymer matrix. MWCNT forms a network throughout the polymer matrix and thus promotes the reinforcement. The rheological studies showed that (for 3 wt% of MWCNTs loading) the material undergoes viscous to elastic transition. At a higher MWCNTs concentration nematic gel-like phase is observed where both storage and loss modulus (G' and G'') are nearly independent of frequency. van Gurp–Palmen plot has been used to determine the viscoelastic properties. Dynamic intersection frequency has been used to correlate the rheological properties with different wt% of MWCNTs loading in ABS. Dynamic rheological measurements revealed the viscous-like ($G'' > G'$) behaviour at a lower MWCNTs loading (<3 wt%) and elastic-like behaviour for higher loading (>3 wt%).

Introduction

Carbon nanotubes (CNTs) due to their small dimensions, low density, large aspect ratio, high mechanical properties and electrical conductivity have attracted great attention. Due to these excellent properties, they have numerous applications [1–3]. Due to these special properties, CNTs are considered excellent candidates for producing high-strength polymer composites [4, 5].

CNT/polymer composites are one of the most potential candidates for commercial applications [6, 7]. Mechanical, electrical properties, thermal stability and flame retardancy of CNT/polymer composites have been studied [8–11]. But the processing of these polymer nanocomposites is a very challenging task [12]. Polymer nanocomposites are different from the traditional nanocomposites due to the significantly enhanced interfacial surface area between the nanoparticles and the polymer chains in the case of polymer nanocomposites. By adding small amount of nanoparticles in the polymer, the percolation takes place. Even a low volume fractions of the reinforcement/filler in the polymer nanocomposites affect the rheological properties significantly. It has been observed that polymer composites containing carbon fibres, single-walled carbon nanotubes [13] (SWCNTs) and multiwalled carbon nanotubes (MWCNTs) show non-terminal solid-like behaviour (viscoelastic) due to the formation of network in the composites. The formation of network structure strongly depends on the concentration of CNTs in the polymer matrix [14–16]. Thus, the rheological properties of

Electronic supplementary material The online version of this article (doi:10.1007/s10853-015-9578-8) contains supplementary material, which is available to authorized users.

✉ Bhanu Pratap Singh
bps@mail.nplindia.org

[1] Physics and Engineering of Carbon, Division of Materials Physics and Engineering, CSIR-National Physical Laboratory, New Delhi 11012, India

[2] Academy of Scientific and Innovative Research (AcSIR), CSIR-National Physical Laboratory, New Delhi 11012, India

[3] Electron and Ion Microscopy Section, CSIR-National Physical Laboratory, New Delhi 11012, India

MWCNTs/polymer composite depend upon its microstructure, state of dispersion, interaction between CNTs and polymer, orientation of nanotubes, aspect ratio etc.

Numerous applications are based on polymeric materials such as electrostatic painting, protective coating etc. Successful preparations of CNT-based composites require proper dispersion of MWCNTs in the polymer, as CNTs have a strong tendency to agglomerate in bundles [17].

Acrylonitrile butadiene styrene (ABS) is a common thermoplastic resin with numerous multi-purpose applications ranging from automotive mouldings and dashboards to aircraft interiors and electronic housings [18]. ABS copolymer is composed of three individual homopolymers: polyacrylonitrile (PAN, a crystalline polymer with high modulus), polybutadiene (BR, an elastomer possessing a low modulus but a high resistance to break) and polystyrene (PS, an inexpensive glassy polymer which is easy to process) [19].

Study of rheological properties of materials is very important. Few studies related to rheological properties of CNT/polymer composites have been reported in literature [1, 20–23]. Potschke et al. [24] studied the effect of nanofiller (carbon black (CB) and MWCNTs) on the electrical, rheological and mechanical properties of melt compounded polycarbonate (PC) composites. Wang et al. [25] studied the effects of modified CNTs with high aspect ratio on the crystallisation kinetics of CNT/isotactic polypropylene (iPP) nanocomposites (with different shear rates and shear times) by using DSC, POM and rheometry. Addition of even a small amount of CNTs in iPP matrix dramatically improved the crystallisation kinetics of CNT/iPP nanocomposites. Above a critical CNT content of 0.1 wt%, a saturation effect is observed which can be correlated to the increased melt viscosity and formation of CNT aggregates at higher CNT contents.

Rostami et al. [26] studied the role of MWCNTs on the rheological, thermal and electrical properties of PC/ABS (75/25) blend prepared by melt blending. Electron microscopic studies revealed that MWCNTs were dispersed quite homogeneously in the PC matrix. The electrical conductivity and electromagnetic interference shielding efficiency of the blend samples got enhanced with increase in the MWCNTs loading. In the study of Bouhfid et al. [27], incorporation of graphene nanosheets in the PA6/ABS blend enhanced the mechanical, electrical and rheological properties. Polyamide 6 (PA6) and acrylonitrile butadiene styrene blend reinforced with graphene nanosheets (GNs) were prepared by batch process followed by hot compression. Addition of even a low amount of graphene (1, 2, 3, 4 wt%) changed the mechanical properties (Young's modulus). The increase in mechanical properties was linear with GNs contents.

Above discussion shows that although there are few reports on the rheological properties of ABS + PC/PA6-based blends with CNTs, but detailed dynamical rheological properties (von Gurp–Palmen plot and dynamic intersection frequency) of MWCNT/ABS composites are not reported. Herein, ABS loaded with various amounts of well-dispersed MWCNTs (1, 3, 5, 7 and 10 wt%) were prepared using micro twin-screw extruder with back flow channel. Dispersion of MWCNTs was studied using SEM and TEM. The effect of different amounts of MWCNTs loading on the rheological properties of MWCNTs/ABS composites is studied. The transition from viscous to elastic behaviour was investigated through the study of complex viscosity with angular frequency, storage modulus and loss modulus with angular frequency and strain, van Gurp–Palmen plot, deflection and damping factor with angular frequency. Further, the mechanical properties of these composites are also studied.

Experimental

Material

MWCNTs were synthesised by catalytic chemical vapour deposition technique. Toluene was used as a hydrocarbon source and ferrocene as a catalyst. The mixture (0.77 g ferrocene in 1 ml of toluene) was fed into heated quartz tube at a feeding rate of 10 ml/h. Details of experimental set-up are given elsewhere [28]. The diameter of MWCNT was in the range of 10–100 nm. The average diameter was 25.8 nm and the average length was 350 μm [29]. ABS used in the present study had a density of 1.068 g/cm^3. It was insoluble in water and soluble in many organic solvents.

Fabrication of MWCNTs/ABS composites

ABS was dried for 10 h at 80 °C in a vacuum oven in order to remove the moisture trapped in the polymer. HAAKE Mini LabII Micro-compounder was used for the dispersion of MWCNTs in ABS. The melt was allowed to flow in the backflow channel of the extruder for 3 min for proper dispersion of CNTs in ABS matrix. After mixing of MWCNTs and ABS matrix in the twin-screw extruder, the mixture was filled into the cylinder and injected into the mould by applying a suitable pressure at the piston. Temperatures of the extrusion and injector were maintained at 260 and 270 °C, respectively [30]. Different MWCNTs/ABS composite samples with varying MWCNTs loadings, i.e. 1, 3, 5, 7, 10 % were prepared and henceforth will be designated as ABS1, ABS3, ABS5, ABS7 and ABS10, respectively. A pure ABS (0 % MWCNTs) sample was also prepared under similar conditions and will be

designated as ABS0. Details of preparation of these composites are shown in Fig. 1.

Morphological characterizations

The dispersion of nanotube bundles in ABS matrix was studied using scanning electron microscope (SEM) and high-resolution transmission electron microscope (HRTEM). Fractured surface of the composites was studied by SEM (model EVO-MA10 ZIESS). HRTEM was carried out using Tecnai G20 S-TWIN, operated at 300 kV and having a point resolution of 0.2 Å.

Rheological measurements

All the rheological measurements were carried out using a controlled-stress rheometer (Rheoplus MCR52 SN81442416) equipped with 25 mm parallel plate geometry. The viscoelastic properties of nanocomposites were investigated at a fixed temperature of 260 °C. Small amplitude oscillatory shear (SAOS) frequency sweep tests were carried out in 0.1–100.0 rad/s range (in the linear viscoelastic regime).

Mechanical properties

For the study of flexural properties, samples with dimensions (length × width × thickness) 70 mm × 12.7 mm × 3.22 mm were prepared. Flexural properties of ABS and MWCNTs/ABS composite were studies using Instron universal testing machine (model 4411) as per the ASTM D790 standard. The span length of the samples was 50 mm and the cross-head speed was at 5 mm/min. The tests were conducted on five samples and the average values with standard deviation are reported.

Results and discussion

Morphological and structural studies

SEM micrographs of ABS1, ABS3, ABS5, ABS7 and ABS10 samples are shown in Fig. 2a–e. CNTs are uniformly dispersed in ABS matrix. These results show that the twin-screw extruder with back flow channel technique is a good technique for obtaining uniform distribution of CNTs in polymer matrix. For further detailed understanding of distribution of CNTs in ABS, TEM studies were carried out.

Figure 3a–c shows the TEM micrographs of sample ABS3 at different magnifications. Well-separated individual CNTs can be seen in TEM micrographs. TEM studies show that even after processing with ABS, CNTs maintain their significant lengths which are good for better stress transfer and improvement in the mechanical properties.

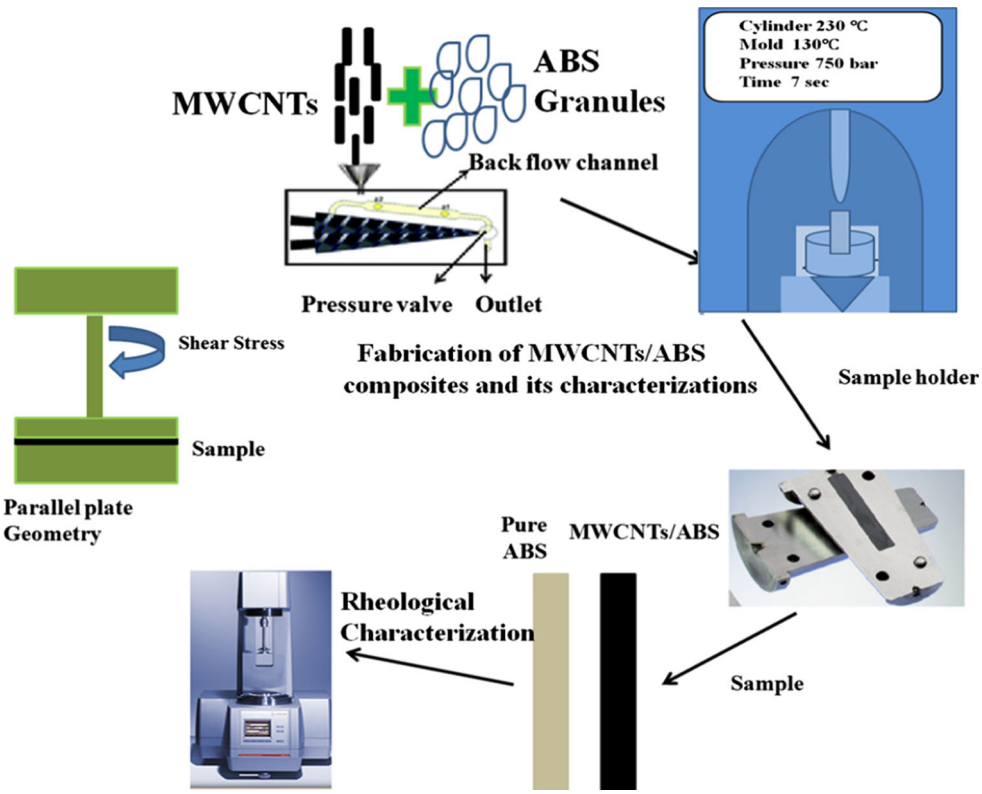

Fig. 1 Schematic diagram showing fabrication of MWCNTs/ABS composites using twin-screw extruder with backflow channel and study of rheological properties

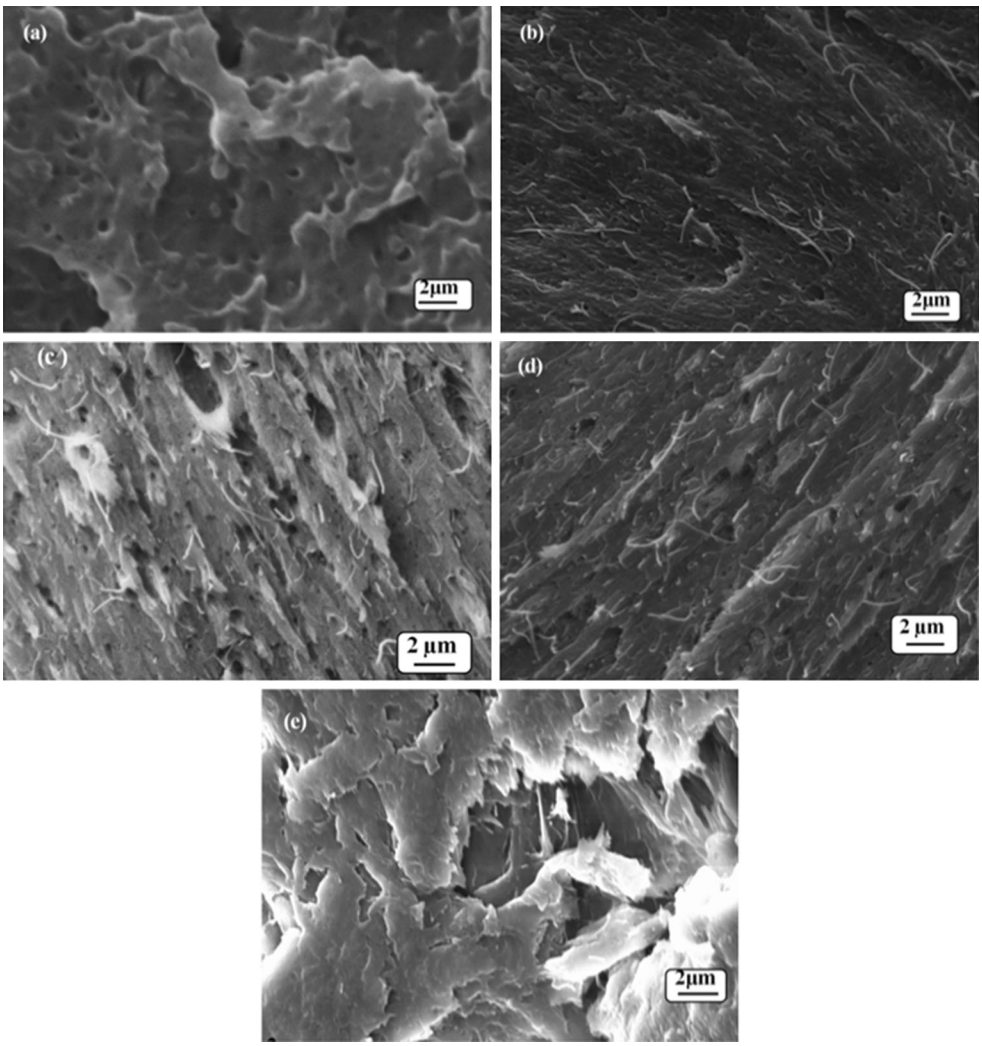

Fig. 2 SEM micrographs of fractured surface of **a** ABS1, **b** ABS3, **c** ABS5, **d** ABS7 and **e** ABS10 composites, respectively

Rheological properties

Figure 4 shows the variation of storage (G') and loss modulus (G'') of composites with strain (at different wt% of MWCNTs loading in ABS). With increase in the loading of MWCNTs G' and G'' increased. With increases in the strain, the value of both modules decreased. The decrease in modulus with increases in strain is due to the change in the structural properties [31].

Variation in storage modulus (G') and loss modulus (G'') (viscoelastic properties) of composites for different wt% of MWCNTs in ABS with frequencies is shown in Fig. 5. At lower frequencies, with increase in wt% of MWCNTs, the values of both G' and G'' increase very sharply (0.1–25 rad/s) and the rate of increase was slower for samples having higher MWCNTs. For ABS0, ABS1 and ABS3 composites, at lower frequencies, ABS chain is fully relaxed and therefore the behaviour is like a terminal behaviour ($G' \approx \omega^2$). ABS0 showed viscous behaviour which is revealed by its stretching from 150 Pa to over 50,000 Pa with change in frequency (as shown in Fig. 5a). With increase in wt% of MWCNTs, terminal behaviour starts disappearing. For samples with higher wt% of MWCNTs, the polymer relaxations get affected and therefore the change in G' and G'' values are not significantly affected. Large change in the storage modulus (G') plot indicates transition from viscous to elastic behaviour [32]. A plateau region below the frequency of 20 rad/s can be seen for samples having CNTs above 5 wt% loading. For samples with higher CNTs, the non-terminal behaviour at lower frequency is due to the formation of an interconnected nanotube network in the polymer matrix.

As reported earlier, with increases in the MWCNTs content in the polymer matrix, a solid-like behaviour is expected. For samples having higher CNTs content, nanotube–nanotube interactions begin to dominate leading to

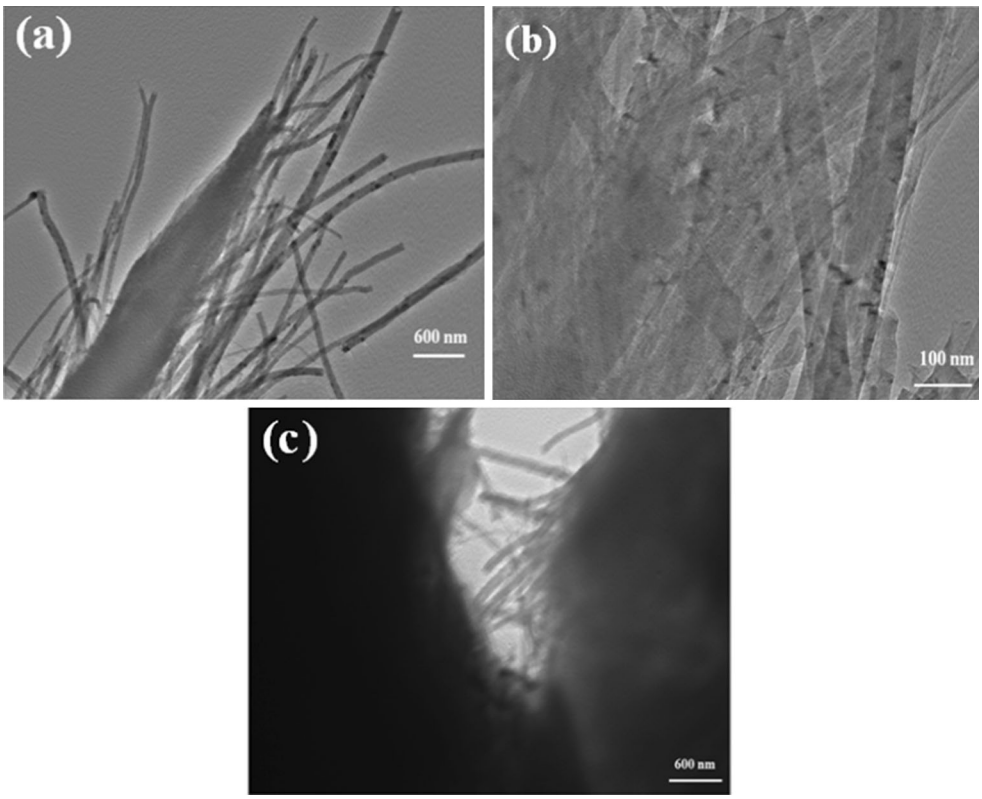

Fig. 3 **a–c** HRTEM micrographs of ABS3 samples at different magnifications

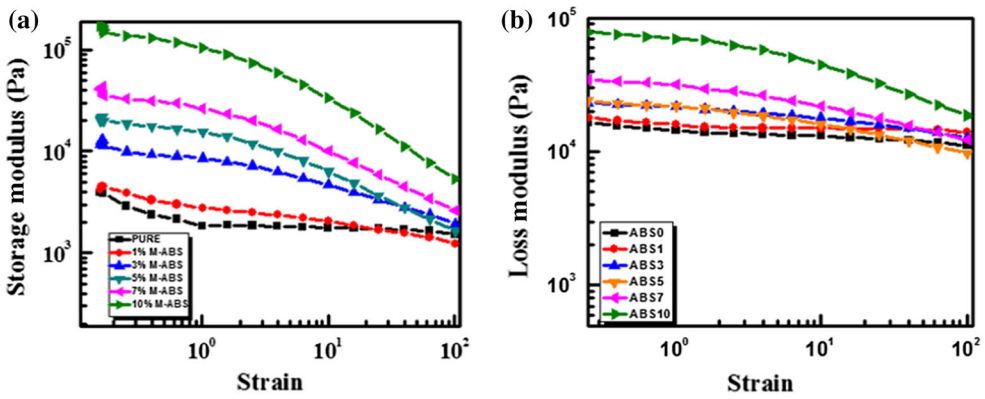

Fig. 4 Variation of **a** storage modulus (G'), and **b** loss modulus (G'') of MWCNTs/ABS composites with strain for varying MWCNTs loading in ABS measured at 260 °C

formation of interconnected structures [1, 33]. At lower frequencies, G'' shows similar trend as G' (Fig. 5b). For samples having same amount of CNTs, G'' increases much slower compared to G'. For ABS0, at lower frequencies, the values of G'' are approximately double to that of G'. For ABS3, G' and G'' values at lower frequencies are equal. For ABS5 and ABS7, the values of G' are twice that of values of G'' due to its non-terminal behaviour. For ABS10, the value of G' is much higher than G''. The limited increase in G'' value with increase in nanofiller content was also reported by Potschke et al. [1]. The change in the slope of modulus curve for ABS3 is significantly greater than other samples, which reveals that transition takes place at 3 wt% loading.

The complex viscosity of ABS0 and composites samples with different wt% of MWCNTs was measured with respect to angular frequency and the results are shown in Fig. 6a. With increase in nanotube's content the complex viscosity increases. At lower frequencies, the effect of nanotube is pronounced and the effect diminished at higher frequencies due to shear thinning behaviour (and thus, the composites behaved like a non-Newtonian) [34–36].

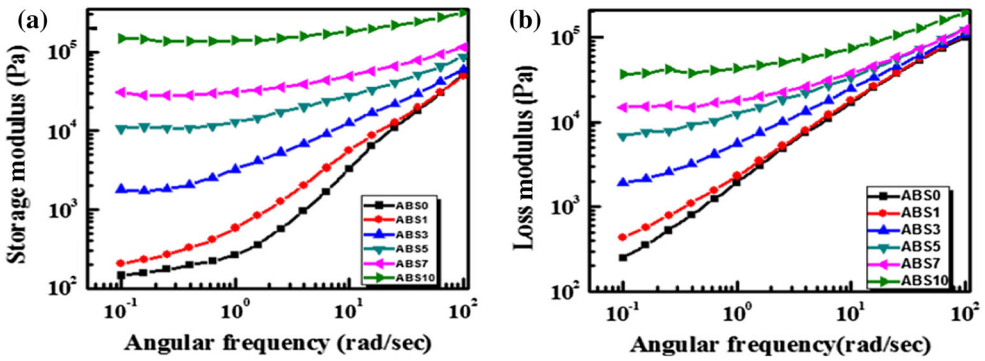

Fig. 5 Variation of **a** Storage modulus (G') and **b** loss modulus (G'') of MWCNTs/ABS composites with frequency sweep for various MWCNTs loading

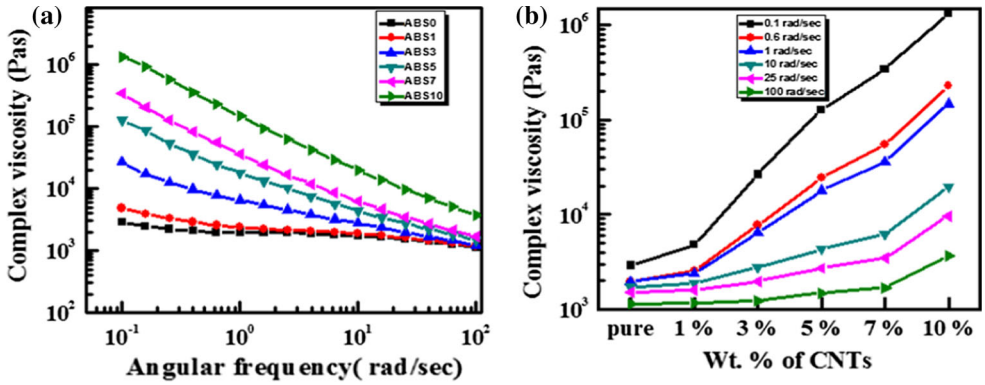

Fig. 6 Variation of **a** complex viscosity $|\eta^*|$ of nanotube-filled ABS composite with frequency, **b** complex viscosity $|\eta^*|$ with various wt% of MWCNTs loading at various frequencies

Figure 6a shows plot of frequencies versus complex viscosity. It can be inferred from Fig. 6a that upon addition of MWCNTs, complex viscosity increased significantly at lower frequency (particularly in samples with higher CNTs loading) indicating restrain in polymer chain relaxation due to the presence of MWCNTs. Fluids for which shearing stress is not linearly related to the rate of shearing strain are designated as non-Newtonian fluids.

ABS0 and ABS1 exhibit only small frequency dependence. Viscosity of ABS10 is three orders of the magnitude greater than that of ABS0. This exhibits strong shear thinning behaviour in ABS10 compared to ABS0.

Figure 6b shows the variation in absolute value of complex viscosity with different wt% of MWCNTs loading. At lower frequencies, the complex viscosity plot is non-linear. A steep slope in the plot for samples ABS0 to ABS3 is observed and the slope becomes almost linear for samples ABS5 to ABS10. From the above result, it can be concluded that with increase in CNTs content, nanotube–nanotube interactions begin to dominate; leading to restrain in the long-range motion of the polymer chains.

Using the vGP-plots, the liquid–solid transition point can be estimated. The vGP-plots for samples with different wt% of MWCNTs are shown in Fig. 7a. For samples ABS0 and ABS1, the curve approaches a phase angle of 90° indicating viscous nature. For ABS3, a small change in the viscous properties is observed. At higher wt% of MWCNTs, the rheological behaviour changes from viscous to elastic (solid) indicating the percolation threshold [37]. For ABS0 and ABS1, the complex modulus lies in the range of 10^3–10^5. For these samples, at higher value of complex modulus, phase angle value starts decreasing indicating viscous behaviour. At lower value of complex modulus a plateau region is observed. Thus, with change in the wt% of MWCNTs loading in ABS matrix, the phase angle changes. The plateau modules can be expressed as [38]

$$G_N^\circ = G(0)\tan\delta \quad (1)$$

When the phase angle is <45°, the behaviour is called elastic. Thus, even by looking at the characteristics value in the vGP-plot, it is the possible to find out whether the polymer is crystalline or amorphous. If the value of phase angle starts decreasing with increase in complex modulus, the material is amorphous. If the material is crystalline in nature, the phase angle starts decreasing with increase in the complex modulus, but after a certain value of complex modulus, the value of the phase angle starts increasing. Thus, ABS and all other samples are amorphous in nature.

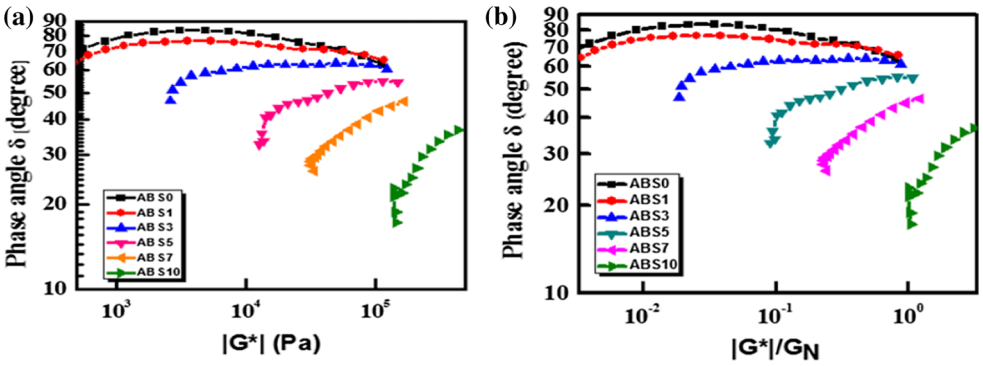

Fig. 7 **a** The vGP-plots of ABS samples with different wt% of MWCNTs, **b** RvGP plots of ABS samples with different wt% MWCNTs in ABS

It has already been reported that the interconnected structure of a filler in a polymeric matrix results in an apparent yield stress [39]. While this effect is visible in dynamic measurements of G' and G'' versus frequency by the presence of a plateau at lower frequency, it can be more pronounced if we plot the complex viscosity versus the complex modulus. It is clear from Fig. 8a that the complex viscosity is independent of complex modulus for samples ABS0 and ABS1. For samples having higher wt% of MWCNTs (i.e. above 3 % wt of MWCNTs), a rapid increase in the complex viscosity with decrease in the complex modulus is observed (Fig. 8a) which indicates the presence of yield stress. Figure 8b shows the plot between strain and shear stress and shows that shear stress increases with increase in MWCNTs wt%.

Figure 9 shows the variation of (a) deflection of nanotube-filled ABS composites and (b) damping factor of nanotube-filled ABS composites with frequency. It can be seen (Fig. 9a) that for samples ABS0 and ABS1, the deflections are larger compared to samples with higher wt% of MWCNTs. The deflection is directly proportional to the applied force or torque. Thus, a large torque was required to create deflection in sample ABS0. For ABS7 and ABS10 samples, the deflection was constant and independent of frequency. This is due to change from viscous to elastic behaviour. After a frequency of 25 rad/s, deflection becomes independent of the CNTs loading.

The damping factor is a useful quantifier of the extent of elasticity of the polymer (after addition of nanofiller). Damping factor greater than one indicates the viscous behavior. Value of damping factor smaller than unity indicates elastic (solid) behaviour. ABS0 and ABS1 showed perfectly viscous behaviour (Fig. 9b). For ABS3 and ABS5 samples, the value of damping factor approaches unity indicating viscoelastic nature. Samples ABS7 and ABS10 showed perfectly elastic behaviour.

Dynamic intersection frequency indicates viscous and elastic behaviour [40–42]. The G' and G'' of the MWCNTs/ABS composites are plotted against frequency and are shown in Fig. 10. For ABS0, the G' and G'' curve do not intersect and they are far away from each other. For ABS0, a shoulder peak was observed in the G' curve which was attributed to the recovery from deformed states. In the lower frequency range, the storage and loss modulus do cross each other leading to increase in relaxation times [43–46]. In the case of ABS0 and ABS1 samples, no intersection point between G' and G'' is observed. For ABS3, the storage and loss modulus curve lies near to each other implying that the viscous behaviour changed due to MWCNTs loading in ABS matrix.

For samples having loads higher than ABS3, G'' is lesser than G' which indicates greater elastic behaviour because of the presence of MWCNTs. For sample ABS5, first a pseudo-solid-like behaviour ($G' > G''$) in the lower

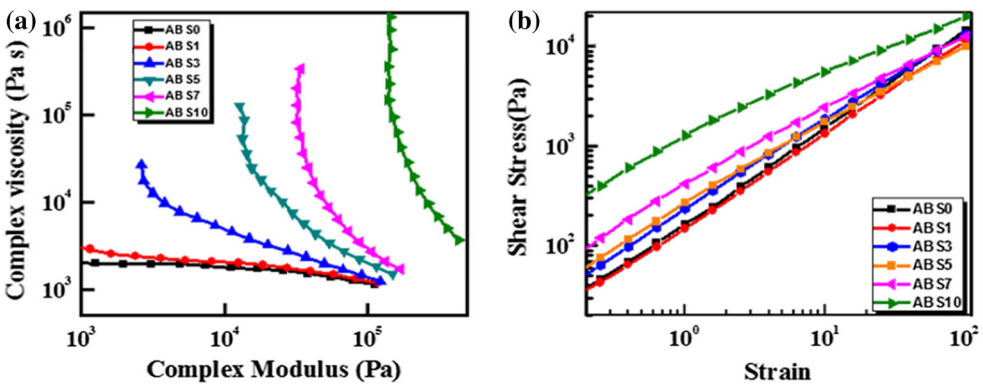

Fig. 8 Variation of **a** complex viscosity versus complex modulus of composites for different wt% of MWCNTs in ABS, and **b** stress versus strain graph for different wt% of MWCNTs

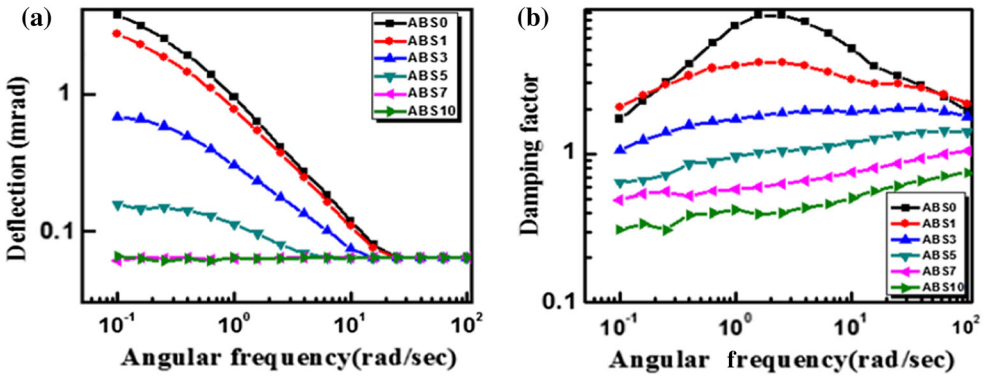

Fig. 9 Variation of **a** deflection of nanotube-filled ABS composites and **b** damping factor of nanotube-filled ABS composites with frequency

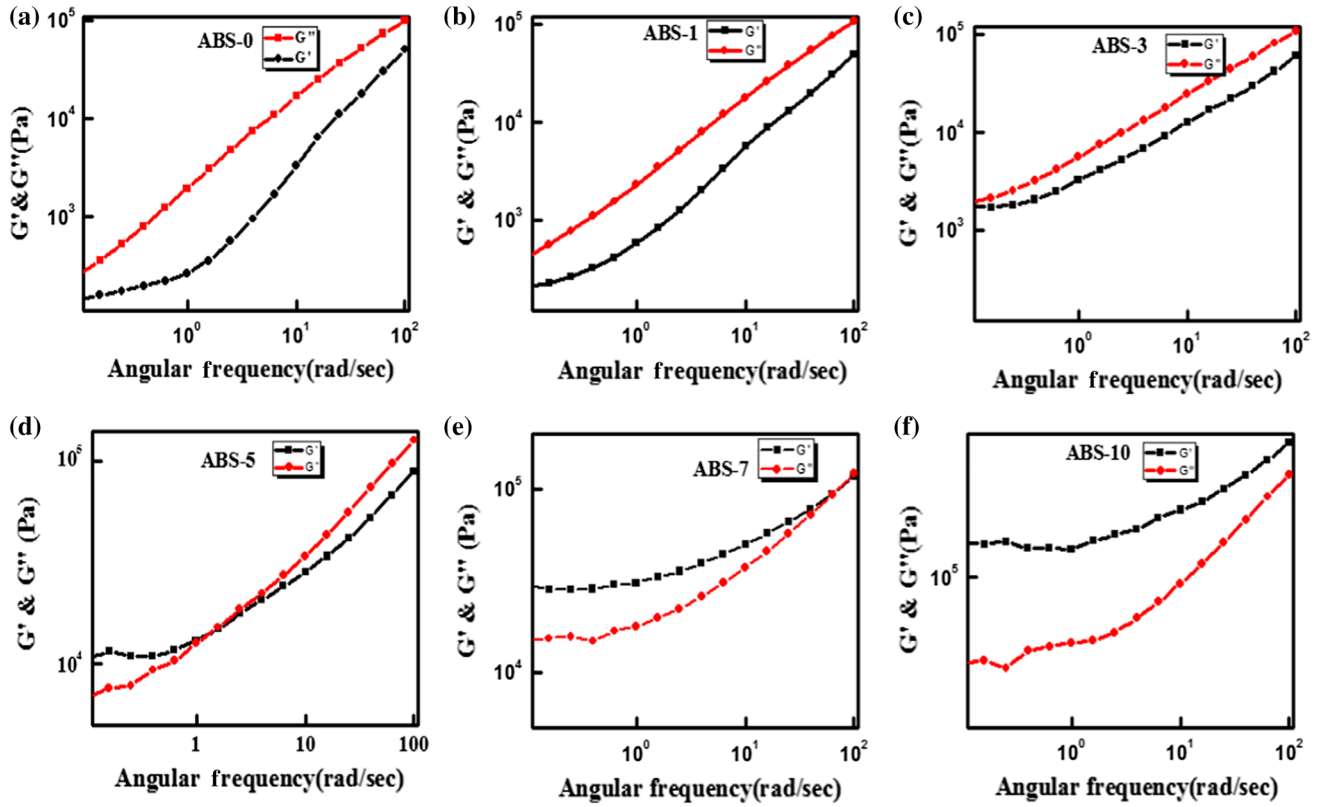

Fig. 10 Plots of storage modulus (G') and loss modulus (G'') with respect to frequencies for various MWCNTs/ABS composite samples

frequency region appears and it gradually becomes pronounced with further increase in MWCNTs content. The pseudo-solid-like behaviour ($G' > G''$) appears only for samples having higher loading of MWCNTs (5 wt%). For sample having still higher wt% (7 %), crossing point of G' and G'' was at higher frequency. In the case of ABS10 sample, in the lower frequency region storage and loss modulus stay far away from each other which indicates that interaction among MWCNTs were dominant.

Further gel nature of these composites is studied which are shown in Fig S1 (see supplementary information).

The increase in viscosity in samples with nanotube (present study) is much higher than the viscosity changes reported for CNF (having larger diameter) and CB composites [1]. This can be due to the higher aspect ratio of the nanotubes. For samples having >3 wt% CNTs loading, transition from viscous to elastic behaviour is observed and have been confirmed by the vGP-plot, dynamic frequency interaction, stress–strain curve, complex viscosity and angular frequency curve. This effect is due to the restriction in polymer chain relaxation due to the presence of MWCNTs in samples having MWCNTs >3 wt%.

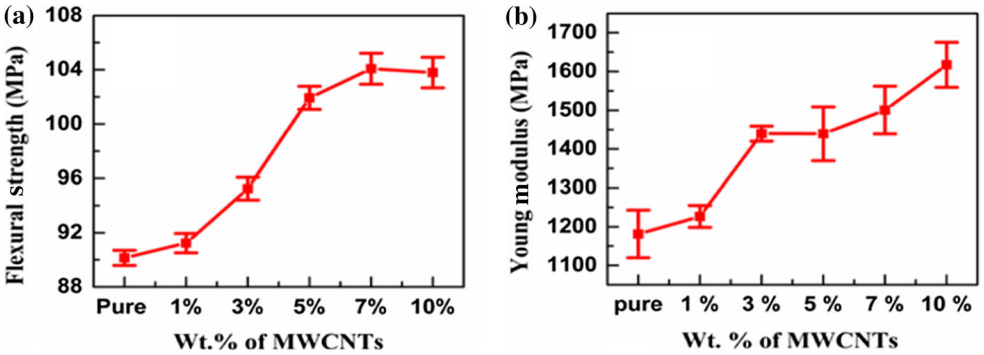

Fig. 11 Flexural properties: **a** flexural strength and **b** flexural modulus

MWCNTs have very good mechanical properties, and therefore their reinforcement in ABS matrix will increase the mechanical properties in a significant way. The mechanical properties in the form of flexural strength, flexural modulus and flexural strain have been studied.

Flexural properties of MWCNTs/ABS composites

Figure 11a shows enhancement in the flexural strength with increase in the MWCNTs loading in ABS polymer. The flexural strength values for samples ABS0, ABS3 and ABS10 are 90.4, 96 and 104 MPa, respectively. The flexural strength for ABS3 and ABS10 were 6 and 13 % higher than ABS0. The flexural strength increased with increase in MWCNT loading (due to proper dispersion of MWCNT in the ABS matrix as confirmed from SEM and TEM images, Figs. 2, 3). Figure 11b shows that the flexural modulus increased with increase in the MWCNTs loading in ABS up to a value of 2504 MPa (ABS7) and then slightly decreased to a value of 2491 MPa (ABS10). Thus, there was 6.7 % enhancement in the flexural strength in sample ABS3 (2204 MPa) compared to ABS0 (2065 MPa). The largest enhancement of 21.2 % in flexural strength was observed in samples ABS7 (compared to sample ABS0).

Conclusions

The investigations on detailed rheological properties of MWCNTs/ABS composites have been carried out. With increase in the concentration of MWCNTs in ABS matrix, the matrix undergoes from dilute to semi dilute and semi dilute to nematic phase. Results of rheological studies showed that the dynamic moduli, viscosity and shear stress increase upon the addition of MWCNTs in ABS. Dynamic rheological measurements revealed that at a lower MWCNTs loading (<3 wt%) the viscous-like ($G'' > G'$) behaviour and for higher loading (>3 wt%) elastic-like behaviour exist. The method of dynamic intersection frequency has been used to explore the crossover frequency between the viscous to elastic region. Additionally, 21.2 % improvement in CNT/ABS composite was observed in the flexural strength values over pure ABS sample. These rheological insights provide valuable information helpful for the commercialization of MWCNT/ABS composites for their application in lightweight and high-strength composites (automotive, computer and equipment housings), antistatic, EMI shielding and energy storage devices.

Acknowledgements The authors wish to express their gratitude to DNPL for his permission to publish the result. The authors would like to thank Miss Preeti for her support in carrying out rheological measurements. Authors are also thankful to Mr. K. N. Sood and Mr. Jay Tawale for SEM measurements. One of the authors (J J) thanks UGC for JRF ship. The research work has been carried out under the CSIR-Network Project (PSC0109).

References

1. Pötschke P, Fornes TD, Paul DR (2002) Rheological behavior of multiwalled carbon nanotube/polycarbonate composites. Polymer 43:3247–3255
2. Han Z, Fina A (2011) Thermal conductivity of carbon nanotubes and their polymer nanocomposites: a review. Prog Polym Sci 36:914–944
3. Singh BP, Choudhary V, Teotia S, Gupta TK, Nand V, Singh VN, Dhakate SR, Mathur RB (2015) Solvent free, efficient, industrially viable, fast dispersion process based amine modified MWCNT reinforced epoxy composites of superior mechanical properties. Adv Mater Lett 6(2):104–113
4. Díez-Pascual AM, Gascón D (2013) Carbon nanotube buckypaper reinforced acrylonitrile–butadiene–styrene composites for electronic applications. ACS Appl Mater Interfaces 5: 12107–12119
5. Chen H, Chen M, Di J, Xu G, Li H, Li Q (2012) Architecting three-dimensional networks in carbon nanotube buckypapers for thermal interface materials. J Phys Chem C 116:3903–3909
6. Spitalsky Z, Tasis D, Papagelis K, Galiotis C (2010) Carbon nanotube–polymer composites: chemistry, processing, mechanical and electrical properties. Prog Polym Sci 35:357–401
7. Pande S, Chaudhary A, Patel D, Singh BP, Mathur RB (2014) Mechanical and electrical properties of multiwall carbon nanotube/polycarbonate composites for electrostatic discharge and electromagnetic interference shielding applications. RSC Adv 4:13839–13849
8. Dalton AB, Collins S, Muñoz E, Razal JM, Ebron VH, Ferraris JP, Baughman RH (2003) Super-tough carbon-nanotube fibres. Nature 423(6941):703

9. Bryning MB, Islam MF, Kikkawa JM, Yodh AG (2005) Very low conductivity threshold in bulk isotropic single-walled carbon nanotube-epoxy composites. Adv Mater 17:1186–1191
10. Babal A, Gupta R, Singh BP, Dhakate SR (2015) Depression in glass transition temperature of multiwalled carbon nanotubes reinforced polycarbonate composites: effect of functionalization. RSC Adv 5:43462–43472
11. Gupta TK, Singh BP, Dhakate SR, Singh VN, Mathur RB (2013) Improved nanoindentation and microwave shielding properties of modified MWCNT reinforced polyurethane composites. J Mater Chem A 1:9138–9149
12. Babal A, Gupta R, Singh BP, Singh VN, Mathur RB, Dhakate SR (2014) Mechanical and electrical properties of high performance MWCNT/polycarbonate composites prepared by an industrial viable twin screw extruder with back flow channel. RSC Adv 4:64649–64658
13. Singh BP, Saket D, Singh A, Pati S, Gupta TK, Singh VN, Mathur RB (2015) Microwave shielding properties of Co/Ni attached to single walled carbon nanotubes. J Mater Chem A 3:13203–13209
14. Bao C, Guo Y, Song L, Kan Y, Qian X, Hu Y (2011) In situ preparation of functionalized graphene oxide/epoxy nanocomposites with effective reinforcements. J Mater Chem 21:13290–13298
15. Yang J, Wang C, Wang K, Zhang Q, Chen F, Du R, Fu Q (2009) Direct formation of nanohybrid shish-kebab in the injection molded bar of polyethylene/multiwalled carbon nanotubes composite. Macromolecules 42(18):7016–7023
16. Love JC, Estroff LA, Kriebel JK, Nuzzo RG, Whitesides GM (2005) Self-assembled monolayers of thiolates on metals as a form of nanotechnology. Chem Rev 105:1103–1169
17. Marceau S, Dubois P, Fulchiron R, Cassagnau P (2009) Viscoelasticity of Brownian carbon nanotubes in PDMS semidilute regime. Macromolecules 42:1433–1438
18. Yang S, Castilleja JR, Barrera E, Lozano K (2004) Thermal analysis of an acrylonitrile–butadiene–styrene/SWNT composite. Polym Degrad Stab 83:383–388
19. Al-Saleh MH, Al-Anid HK, Husain YA, El-Ghanem HM, Jawad SA (2013) Impedance characteristics and conductivity of CNT/ABS nanocomposites. J Phys D 46:385305–385313
20. Bauhofer W, Kovacs JZ (2009) A review and analysis of electrical percolation in carbon nanotube polymer composites. Compos Sci Technol 69:1486–1498
21. Liang G, Tjong S (2006) Electrical properties of low-density polyethylene/multiwall carbon nanotube nanocomposites. Mater Chem Phys 100:132–137
22. Pötschke P, Bhattacharyya AR, Janke A (2004) Carbon nanotube-filled polycarbonate composites produced by melt mixing and their use in blends with polyethylene. Carbon 42:965–969
23. Chatterjee T, Krishnamoorti R (2013) Rheology of polymer carbon nanotubes composites. Soft Matter 9:9515–9529
24. Poetschke P, Arnaldo MH, Radusch H-J (2012) Percolation behavior and mehanical properties of polycarbonate composites filled with carbon black/carbon nanotube systems. Polimery 57:204–211
25. Wang J, Yang J, Deng L, Fang H, Zhang Y, Wang Z (2015) More dominant shear flow effect assisted by added carbon nanotubes on crystallization kinetics of isotactic polypropylene in nanocomposites. ACS Appl Mater Interfaces 7:1364–1375
26. Rostami A, Masoomi M, Fayazi MJ, Vahdati M (2015) Role of multiwalled carbon nanotubes (MWCNTs) on rheological, thermal and electrical properties of PC/ABS blend. RSC Adv 5:32880
27. Bouhfid R, Arrakhiz FZ, Qaiss A (2014) Effect of graphene nanosheets on the mechanical, electrical, and rheological properties of polyamide, 6/acrylonitrile–butadiene–styrene blends. Polym Compos. doi:10.1002/pc.23259
28. Mathur RB, Chatterjee S, Singh BP (2008) Growth of carbon nanotubes on carbon fibre substrates to produce hybrid/phenolic composites with improved mechanical properties. Compos Sci Technol 68:1608–1614
29. Singh BP, Saini K, Choudhary V, Teotia S, Pande S, Saini P, Mathur RB (2014) Effect of length of carbon nanotubes on electromagnetic interference shielding and mechanical properties of their reinforced epoxy composites. J Nanopart Res 16: 2161–2172
30. Jyoti J, Basu S, Singh BP, Dhakate SR (2015) Superior mechanical and electrical properties of multiwall carbon nanotube reinforced acrylonitrile butadiene styrene high performance composites. Compos B 83:58–65
31. Payne A, Whittaker R (1971) Low strain dynamic properties of filled rubbers. Rubber Chem Technol 44:440–478
32. Seo M-K, Park S-J (2004) Electrical resistivity and rheological behaviors of carbon nanotubes-filled polypropylene composites. Chem Phys Lett 395:44–48
33. Abdel-Goad M, Pötschke P, Zhou D, Mark JE, Heinrich G (2007) Preparation and rheological characterization of polymer nanocomposites based on expanded graphite. J Macromol Sci Part A 44:591–598
34. White JL, Czarnecki L, Tanaka H (1980) Experimental studies of the influence of particle and fiber reinforcement on the rheological properties of polymer melts. Rubber Chem Technol 53:823–835
35. Czarnecki L, White JL (1980) Shear flow rheological properties, fiber damage, and mastication characteristics of aramid-, glass-, and cellulose-fiber-reinforced polystyrene melts. J Appl Polym Sci 25:1217–1244
36. Van Krevelen DW, Te Nijenhuis K (2009) Properties of polymers: their correlation with chemical structure; their numerical estimation and prediction from additive group contributions. Elsevier, Amsterdam
37. Prashantha K, Soulestin J, Lacrampe M, Krawczak P, Dupin G, Claes M (2009) Masterbatch-based multi-walled carbon nanotube filled polypropylene nanocomposites: assessment of rheological and mechanical properties. Compos Sci Technol 69:1756–1763
38. Trinkle S, Friedrich C (2001) Van Gurp-Palmen-plot: a way to characterize polydispersity of linear polymers. Rheol Acta 40:322–328
39. Ceccia S, Ferri D, Tabuani D, Maffettone PL (2008) Rheology of carbon nanofiber-reinforced polypropylene. Rheol Acta 47:425–433
40. Chen Y, Li H (2005) Phase morphology evolution and compatibility improvement of PP/EPDM by ultrasound irradiation. Polymer 46:7707–7714
41. Oprea V, Simonescu C (1973) Mechonochemical reactions of PE-epsilon-block copolymerization of PE with polycaprolactam by vibratory grinding. Plaste Kayt 20:174–179
42. Ezzati P, Ghasemi I, Karrabi M, Azizi H (2008) Rheological behaviour of PP/EPDM blend: the effect of compatibilization. Iran Polym J 17:669–679
43. Li R, Yu W, Zhou C (2006) Phase behavior and its viscoelastic responses of poly (methyl methacrylate) and poly (styrene-co-maleic anhydride) blend systems. Polym Bull 56:455–466
44. Li R, Yu W, Zhou C (2006) Rheological characterization of droplet-matrix versus co-continuous morphology. J Macromol Sci Part B 45:889–898
45. Macaubas P, Demarquette N (2001) Morphologies and interfacial tensions of immiscible polypropylene/polystyrene blends modified with triblock copolymers. Polymer 42:2543–2554
46. Sung Y, Han M, Hyun J, Kim W, Lee H (2003) Rheological properties and interfacial tension of polypropylene–poly (styrene-co-acrylonitrile) blend containing compatibilizer. Polymer 44: 1681–1687